

# Fe<sup>0</sup> Nanoparticles Remain Mobile in Porous Media after Aging Due to Slow Desorption of Polymeric Surface Modifiers

HYE-JIN KIM,<sup>†,‡</sup> TANAPON PHENRAT,<sup>†,‡</sup> ROBERT D. TILTON,<sup>\*,§,‡</sup> AND GREGORY V. LOWRY<sup>\*,†,§,‡</sup>

Department of Civil and Environmental Engineering, Department of Chemical Engineering, Department of Biomedical Engineering, and Center for Environmental Implications of NanoTechnology (CEINT), Carnegie Mellon University, Pittsburgh, Pennsylvania 15213-3890

Received October 24, 2008. Revised manuscript received March 31, 2009. Accepted April 1, 2009.

Nanosized zerovalent iron (nZVI) is used for in situ remediation of contaminated groundwater. Polyelectrolyte surface coatings are used to inhibit nZVI aggregation and enhance mobility in the subsurface for emplacement. The fate of nZVI is of interest given the uncertainties regarding the effects of nanomaterials on the environment, and depends in part on the stability of these surface coatings against desorption and biodegradation. This study measured the rate and extent of desorption of polyelectrolyte coatings used to stabilize nZVI, including polyaspartate (PAP MW = 2.5 kg/mol and 10 kg/mol), carboxymethyl cellulose (CMC MW = 90 kg/mol and 700 kg/mol), and polystyrene sulfonate (PSS MW = 70 kg/mol and 1000 kg/mol). The initial adsorbed mass of polyelectrolyte ranged from 0.85 to 3.71 mg/m<sup>2</sup> depending on the type and molecular weight (MW). Polyelectrolyte adsorption was confirmed by an increase in nZVI electrophoretic mobility. In all cases, desorption of polyelectrolyte was slow, with less than 30 wt% desorbed after 4 months. The higher MW polyelectrolyte had a greater adsorbed mass and a slower desorption rate for PAP and CMC. nZVI mobility in sand columns after 8 month of desorption was similar to freshly modified nZVI, and significantly greater than unmodified nZVI aged for the same time under identical conditions. Based on these results, polyelectrolyte modified nanoparticles will remain more mobile than their unmodified counterparts even after aging. Other factors potentially affecting the fate of coated nZVI must be evaluated, especially the potential for biodegradation of coatings.

## Introduction

Reactive Fe<sup>0</sup> nanoparticles, or nZVI, are used for remediation of groundwater contaminated with chlorinated solvents and heavy metals (1) because they can be applied in situ (2, 3), have a high surface to volume ratio and hence high reactivity

with contaminants (4), and are relatively resistant to fouling from groundwater constituents (5, 6). Typically, nZVI is injected into the contaminant source zone and left in place (7). Mounting concerns over the effects of manufactured nanomaterials on environmental health and safety make it prudent to determine the fate of injected nZVI (8, 9). Most manufactured nanomaterials, including nZVI used for aquifer remediation, have engineered polymeric coatings. These coatings significantly affect their mobility in the environment so understanding the persistence of these coatings is essential to determining their environmental fate.

nZVI particles consist of a Fe<sup>0</sup> core and predominantly magnetite (iron oxide) shell. The mobility of bare (uncoated) nZVI in the subsurface is limited by its rapid aggregation and subsequent nZVI deposition onto aquifer media (2, 3, 10). To improve mobility, nZVI is either supported onto larger particles (e.g., activated carbon supported nZVI (11) whose surfaces are modified, or the nZVI surface is directly modified to stabilize the nanoparticles against aggregation (3, 12–15). Anionic polyelectrolytes, including polyaspartate (PAP), carboxymethyl cellulose (CMC), and polystyrene sulfonate (PSS) (12, 13) are effective surface modifiers that provide electrosteric stabilization against aggregation and reduce nZVI deposition onto aquifer materials through electrosteric repulsion with negatively charged soil minerals (15). They also can decrease nZVI reactivity by a factor of 4–20 depending on the type of coating and on the adsorbed amount (2, 16).

Polymers adsorb onto particle surfaces when the loss of translational and configurational entropy upon adsorption is compensated by a favorable energy of adsorption (17). Because they are flexible chains, polymers adsorb with many points of adsorption per chain, leading to high overall adsorption energies, strong adsorption, and slow desorption (17). Adsorbed chains can be replaced slowly on the surface by other chains in solution, or displaced by increasing concentrations of electrolytes or other solutes, but desorption into polymer-free solvent is usually so slow that adsorption is effectively irreversible on laboratory time scales (18). This has been attributed to extreme limitations on the diffusion of polymers with high adsorption affinity away from the surface (17, 19). Polymer adsorption on solids can be either physisorption, where the polymer-surface interaction is dispersive or electrostatic in nature, or chemisorption, where specific functional groups form covalent bonds with the surface. Chemisorption is an extreme case where covalent bonds make the adsorption irreversible (20), but polymer physisorption often produces sufficiently large adsorption energies of several kT per monomer as to make the adsorption effectively irreversible (19). Higher molecular weight (MW) polyelectrolytes should have higher adsorption energy, and therefore desorb more slowly than lower MW polyelectrolytes of the same monomer.

Polyelectrolyte adsorption is controlled by a delicate balance of competing factors, including electrostatic attraction of segments and oppositely charged surfaces, and electrostatic repulsions among neighboring polyelectrolyte segments. These are often augmented by nonelectrostatic attraction between the polyelectrolyte and the surface (17, 18, 21). The latter are particularly important for polyelectrolyte adsorption to similarly charged surfaces (22). PSS homopolymers adsorb to iron oxide surfaces, accompanied by proton coadsorption. This charge regulation yields a significant increase in the positive charge density of the underlying surface and an increase in the point of zero charge to higher pH (23). Azo dye adsorption experiments have

\* Corresponding author phone: 412-268-2948; fax: 412-268-7813; e-mail: glowry@cmu.edu.

<sup>†</sup> Department of Civil and Environmental Engineering.

<sup>‡</sup> Center for Environmental Implications of NanoTechnology (CEINT).

<sup>§</sup> Department of Chemical Engineering.

<sup>§</sup> Department of Biomedical Engineering.

shown that sulfonate groups may form specific bidentate or unidentate linkages to iron oxides in a strongly pH dependent manner (24), although the extent to which this governs PSS adsorption to iron oxides is unknown. Specific bidentate linkages between carboxyls and iron oxides has been shown to drive carboxylated polyelectrolyte adsorption to iron oxides (25, 26), making this an important mechanism for PAP and CMC adsorption to nZVI. The desorption rate should therefore depend on the monomer type via the specific interaction afforded by the monomer.

Adsorption of carboxylated polyelectrolytes to metal oxides or other minerals is often considered irreversible (27, 28), however, desorption into polymer-free solutions is typically only monitored over the course of hours to weeks (29, 30). Here we examine polyelectrolyte desorption from nZVI into polyelectrolyte-free solutions for electrolyte conditions and months long time scales that are relevant to in situ groundwater remediation where desorption may be significant. Desorption of polymeric stabilizers from nZVI has not been studied previously on any time scale.

The goal of this study is to determine the effect of molecular weight and common types of polyelectrolyte functionality (weak polyelectrolytes with charge arising from titratable carboxyls and strong polyelectrolytes with nontitratable sulfonate groups) on the rate and extent of desorption from nZVI over several months. PAP (MW = 2.5 K and 10 K), CMC (MW = 90 K and 700 K), and PSS (MW = 70 K and 1 M) were chosen as model polyelectrolyte stabilizers for nZVI. The mass of polyelectrolyte desorbed into initially polymer-free 1 mM NaHCO<sub>3</sub> solution was monitored for four months. The desorption results were complemented by measurements of nZVI electrophoretic mobility (EPM), stability against aggregation after desorption, and transport through saturated sand columns in order to establish the colloidal consequences of stabilizer desorption. Freshly modified nZVI and bare, but aged nZVI served as experimental controls.

## Materials and Methods

**Nanoparticles.** nZVI with a Fe<sup>0</sup> core and Fe<sub>3</sub>O<sub>4</sub> outer shell (reactive nanoscale iron particles, RNIP) was obtained from Toda Kogyo, Japan. RNIP is a polydisperse suspension of irregularly shaped particles, with primary particles ranging in size from 5 to 70 nm with a median radius of ~20 nm. Detailed physical and chemical properties of RNIP have been reported previously (4, 10, 31). RNIP was stored anaerobically as a concentrated aqueous slurry (300 g/L) in a sealed container at high pH (pH 10.6) where Fe<sup>0</sup> oxidation is minimized. H<sub>2</sub> generation measurements (4) indicated that the Fe<sup>0</sup> content of the stock slurry was 45% (w/w) when this experiment was conducted. A RNIP stock solution (120 g/L) was prepared in 1 mM sodium bicarbonate (NaHCO<sub>3</sub>) buffer and sonicated (model 550 sonic dismembrator, Fisher Scientific, Howell, NJ) to break aggregates formed during storage. The sonicated stock was diluted again with 1 mM NaHCO<sub>3</sub> to 3 g/L. The total Fe concentration in each stock solution was determined by atomic absorption spectrometry (GBC at 248.3 nm within the range of 0–10 mg/L Fe) after acid digestion in concentrated HCl (trace metal grade) as previously described (2, 10).

**Polyelectrolytes.** Sodium poly(aspartate), an anionic polypeptide and weak polyelectrolyte, with molecular weights of 2~3 kg/mol (PAP2.5K) and 10 kg/mol (PAP10K) were from Lanxess and NanoChem Solutions Inc., respectively. Sodium poly(styrene sulfonate), an anionic strong polyelectrolyte with molecular weights of 70 kg/mol (PSS70K) and 1000 kg/mol (PSS1M), and sodium carboxymethyl cellulose, an anionic polysaccharide, and weak polyelectrolyte with molecular weights of 90 kg/mol (CMC90K) and 700 kg/mol (CMC700K) were from Aldrich. Chemical properties and structures of these polyelectrolytes are provided in ref 12.

**Polyelectrolyte Adsorption and Desorption.** Adsorption to RNIP nZVI was measured by solution depletion in 24 mL suspensions containing 3 g/L nZVI and 1 g/L of the polyelectrolyte at 25 °C. The pH of these suspensions was pH 9.5 after 5 days of equilibrium time. At this pH, nZVI and the anionic polyelectrolytes are both negatively charged (Supporting Information Figure S1). The ratio of particle surface area to polyelectrolyte concentration provides the maximum adsorbed mass at these conditions (12, 16). After 5 days of mixing on an end-over-end rotator at 30 rpm, the particle suspensions were ultracentrifuged at 68,400g for 80 min (Sorvall ultracentrifuge OTD65B). The polyelectrolyte concentration in the supernatant was measured by UV–vis spectrophotometry (Varian Palo Alto, CA) for PSS, and by a total organic carbon analyzer (OI Analytical) for PAP and CMC as described in ref 12. PSS was quantified from the difference in absorbance at 225 nm and at 212 nm as a function of PSS concentration to minimize the interference by iron. For total organic carbon analysis, five calibration standards ranging from 1 to 100 mg/L in 1 mM NaHCO<sub>3</sub> provided a linear response. Supernatant samples were diluted if necessary to remain in this linear calibration range. The adsorbed mass was calculated from the difference between the initial and equilibrium concentration of dissolved polyelectrolyte, normalized by the RNIP specific surface area. The latter was determined by the N<sub>2</sub>–BET method to be 15 m<sup>2</sup>/g for this sample. Triplicate samples were prepared for each polyelectrolyte, and the results are reported as the mean ± one standard deviation.

After quantifying the adsorbed polyelectrolyte mass, excess polyelectrolyte was removed from the solution by centrifuging, decanting (20 of 24 mL each time), and refilling with polyelectrolyte-free 1 mM NaHCO<sub>3</sub> solution four times. This procedure decreased the concentration of nonadsorbed polyelectrolyte in the solution to <1 mg/L. The washed particles were rotated end-over-end at 30 rpm and 25 °C. It was assumed that polyelectrolyte degradation was negligible. The suspensions were centrifuged and the supernatant was analyzed for desorbed polyelectrolyte after 2, 4 to 6, 8, and 16 weeks. The same volume of polyelectrolyte-free 1 mM NaHCO<sub>3</sub> was replaced each time to make up for the sampled volume. Control experiments (method blank) were conducted identically but without polyelectrolyte to monitor changes in bare nZVI due to centrifugation, washing and aging.

**Particle Surface Chemistry.** The electrophoretic mobility (EPM) of bare and modified nZVI was measured as a function of pH (pH 2~10) to monitor the change in surface charge due to polyelectrolyte adsorption and desorption. Freshly polyelectrolyte-modified nZVI was measured with nonadsorbed polyelectrolyte in the solution to ensure that the maximum possible adsorbed amount was present on the nZVI. Measurements made after 8 and 16 weeks of desorption did not contain any free polyelectrolyte. EPM was measured on dilute dispersions (~15 mg/L) in 5 mM NaHCO<sub>3</sub> using a Malvern Zetasizer 3000 (Southborough, MA). pH was adjusted by adding NaOH (0.1 or 0.01 N) or HCl (0.1 or 0.01 N) as needed. Samples were sonicated in a water bath (Bransonic 2510) for 5 min just prior to EPM measurement.

**Sedimentation.** The colloidal stability of freshly modified particles and particles aged over 8 months of desorption was assessed by monitoring the sedimentation of an 800 mg/L particle suspension at 25 °C with UV–vis (508 nm) spectrophotometry (Varian, Palo Alto, CA) for 50 min as described in ref 12. Samples were sonicated in a water bath for 5 min before the measurement.

**Transport Experiments.** Transport studies were performed in water-saturated silica sand ( $d_p = 300 \mu\text{m}$ ) in stainless steel columns (12.5 cm length  $\times$  1.25 cm o.d.) as described in ref 2. Columns were packed wet and flushed with a 1 mM NaHCO<sub>3</sub> solution for at least 10 pore volumes

**TABLE 1. Initial Adsorbed Mass (mg/m<sup>2</sup>), Percent Remaining during the 4-Month Desorption Period and Estimated First-order Desorption Rate Constant**

time	initial adsorbed mass (mg/m <sup>2</sup> ) <sup>a</sup>	2 weeks <sup>a</sup> (% remaining)	4 weeks <sup>a</sup> (% remaining)	8 weeks <sup>a</sup> (% remaining)	16 weeks <sup>a</sup> (% remaining)	desorption rate constant (first order)	
						rapid <sup>b</sup> (1/day × 10 <sup>3</sup> )	slow <sup>c</sup> (1/day × 10 <sup>3</sup> )
PAP2.5K	0.85 ± 0.2	90.9 ± 3.0	86 ± 4.7	81.7 ± 5.5	73.9 ± 8.1	6.0 ± 1.9	1.9 ± 0.9
PAP10K	1.47 ± 0.1	94.5 ± 2.3	91.5 ± 2.5	90.0 ± 2.0	87.2 ± 2.8	3.5 ± 1.5	0.59 ± 0.12
time	0	2 weeks	5 weeks	8 weeks	16 weeks	rapid (1/day)	slow (1/day)
PSS70K	2.89 ± 0.6	94.3 ± 0.5	93.5 ± 0.6	93.5 ± 0.6	93.5 ± 0.6	3.7 ± 0.3	
PSS1M	2.55 ± 0.5	95.9 ± 4.1	95.1 ± 4.7	95.1 ± 4.7	95.1 ± 4.7	2.7 ± 2.7	
time	0	2 weeks	6 weeks	8 weeks	16 weeks	rapid (1/day)	slow (1/day)
CMC90K	2.09 ± 0.0	87.6 ± 2.1	83.1 ± 2.9	81.1 ± 3.1	79.7 ± 3.3	8.3 ± 1.5	0.53 ± 0.09
CMC700K	3.71 ± 0.4	93.8 ± 0.4	91.5 ± 0.8	90.4 ± 0.9	89.6 ± 1.2	4.0 ± 0.3	0.27 ± 0.06

<sup>a</sup> Values were measured from triplicate samples. <sup>b</sup> Rapid desorption rate is from linear regression of the initial two points. Errors are standard deviation of triplicate measurements. <sup>c</sup> Slow desorption rate is from the linear regression of the last three points. Errors are standard deviation of triplicate measurements.

(PV) to obtain a uniform surface charge on the sand. The porosity was 0.33 and the linear pore water velocity was maintained at 0.11 cm/s with a peristaltic pump. A square pulse (2 min; 4 mL; 1 PV) of particles at 1 g/L was introduced into the column. During injection, the particle suspension source reservoir was sonicated with an ultrasonic probe to minimize aggregation and sedimentation prior to introducing them into the column. Column effluent was collected for 12 pore volumes. An aliquot of the effluent was dissolved in HCl (1 to 2 vol/vol ratio), diluted with 1% HNO<sub>3</sub> and analyzed for total iron using flame atomic absorption spectrometry (GBC 908 AA). The influent particle concentration was measured the same way. Since polyelectrolyte coatings significantly enhance nZVI elutability from such sand columns, any detriment in nZVI elutability between freshly coated and aged particles would be attributable to polyelectrolyte layer changes during desorption. It is possible that slow reconfigurations of adsorbed polyelectrolytes could also modify nZVI elutability. Aging of nZVI alone can affect the aggregation and transport of RNIP because oxidation decreases the Fe<sup>0</sup> content and thus the magnetic attraction between particles decreases (10). To account for these changes, controls using bare but identically handled nZVI were run to monitor possible colloidal changes due simply to nZVI aging.

## Results and Discussion

**Adsorption and Desorption.** The initial adsorbed mass is provided in Table 1 for each polyelectrolyte. The surface excess concentrations ranged from 0.85 to 3.7 mg/m<sup>2</sup> depending on the type and molecular weight of polyelectrolyte. For PAP and CMC, the higher molecular weight polyelectrolyte showed higher adsorption. Among three types of polyelectrolytes, the adsorbed mass of PAP, which has the smallest molecular weight, was generally less than for PSS and CMC. The dependence of polyelectrolyte adsorption on the degree of polymerization (molecular weight) is subtle and depends on the delicate balancing of forces at work during adsorption (17). While the extent of electrostatically driven polyelectrolyte adsorption is known to depend very weakly on molecular weight (31–36), this may not be the case for adsorption against a net electrostatic repulsion. Chibowski and Wisniewska (37) observed increased adsorption for increasing molecular weight for carboxyl function-

alized anionic polyelectrolytes on net negatively charged hematite, similar to the current observation. The increased adsorption was attributed to an increased number and size of adsorbed loops for higher molecular weight polyelectrolytes. The molecular weight independence of the PSS adsorbed mass on nZVI was previously observed by this group (12).

Polyelectrolyte desorption was monitored from the appearance of the free polyelectrolyte in supernatant solutions over a four month period (Table 1). Less than 30% of adsorbed polyelectrolytes were desorbed from the particles after four months. PAP2.5K, CMC90K, PSS70K, which are the lower molecular weight samples of each polyelectrolyte, showed 2–9% more desorption than the same polyelectrolyte with higher molecular weight. It is well established that high molecular weight polymers have a higher affinity due to the increased number of attachment points per chain, so this result is expected.

Whereas PAP and CMC desorbed by as much as ~30%, PSS desorbed only ~4–6% for either molecular weight. As noted above, the extent to which specific sulfonate bidentate or unidentate linkages to the surface may influence PSS adsorption is unknown. It is notable that electrostatic repulsions inhibit these linkages for sulfonated small molecule dyes at higher pH near the point of zero charge of the iron oxide (24). It is possible that the polymeric nature of PSS may allow some segments to locate isolated protonated FeO groups on the nZVI surface, an effect that might be promoted by proton coadsorption noted above. Adsorption of the relatively hydrophobic backbone of PSS to the surface may be involved as well. These hypotheses remain to be tested. In any case, of comparison similarly sized PSS and CMC results suggests that the nonelectrostatic interactions that drive PSS adsorption provide a greater resistance to desorption from negatively charged nZVI than do the carboxyl linkages that promote CMC adsorption. PAP showed the greatest amount of desorption. This may be due to the multilayer adsorption configuration of PAP onto nZVI (12). Desorption was bimodal, beginning at a relatively larger rate (from time = 0–2 weeks), and slowing considerably (from time = 4–16 weeks). Treating the first and second stages of desorption as pseudofirst order processes gave apparent desorption rate constants of 10<sup>-3</sup>–10<sup>-4</sup>/day. Desorption rate constants were obtained separately for the “rapid” desorption

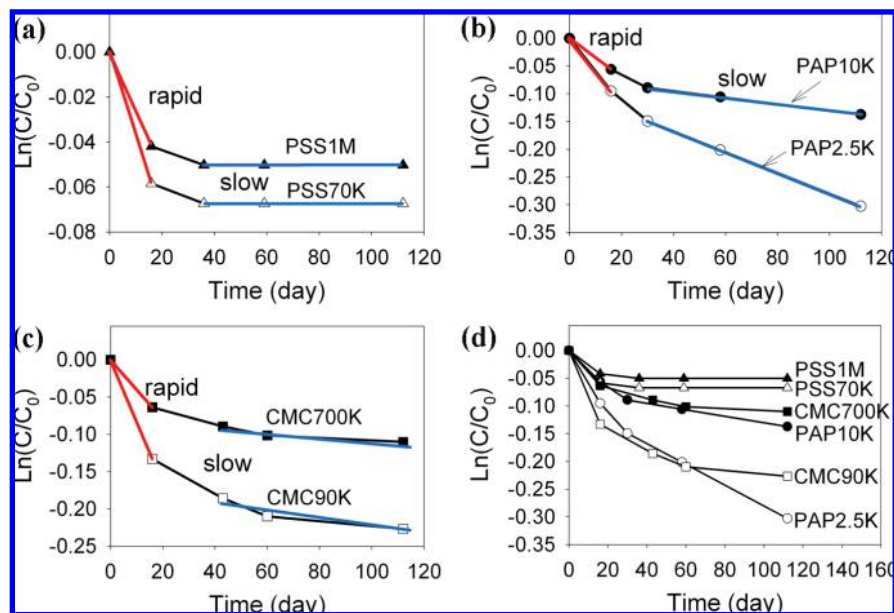


**FIGURE 1.** Desorption of (a) PSS (low MW ( $\Delta$ ), high MW ( $\blacktriangle$ )), (b) PAP (low MW ( $\circ$ ), high MW ( $\bullet$ )), (c) CMC (low MW ( $\square$ ), high MW ( $\blacksquare$ )) and (d) all of the polyelectrolytes tested from RNIP during a 4-month period. Linear regression for the initial two points (rapid) and last three points (slow) were done separately. Data points are the average of triplicate samples.

regime and “slow” desorption regime (Table 1, Figure 1). PSS showed the lowest desorption rate among the three polymers and the slow desorption step was not measurable because the desorbed mass was not detectable. The desorption rates of PAP and CMC were similar despite their difference in molecular weight and composition. Based on the assumption that the first order desorption rate constant in the slow desorption region is constant with time, the desorption half-lives for PAP and CMC range from 1 to 6 years. Sukhishvili and Granick (38) also observed a fast desorption step followed by slow desorption of poly(1,4 vinyl) pyridine (PVP) from the silicon oxide surface at low ionic strength. The polyelectrolytes used here, and most commercially available polymers or polyelectrolytes, are poly-disperse and have a distribution of molecular weights. As such, the initial rapid desorption might be attributable to the shorter and therefore more weakly bound chains while the slow desorption regime may be attributable to the longer chains with stronger overall binding to the surface.

**Effect of Polyelectrolyte Adsorption and Desorption on nZVI Surface Charge.** The EPM of nZVI in the presence of excess polymer was always more negative than bare nZVI over the entire pH range, indicating that the negatively charged polyelectrolytes indeed adsorbed to the negatively charged nZVI surface (Figure 2a–c and Supporting Information Figure S1). The isoelectric point for the uncoated RNIP was  $\sim$ pH<sub>iep</sub> 6.3 (Figure 2(d)). Falling within the range of pH<sub>iep</sub> (pH 6.0–6.8) reported for magnetite (25), this is consistent with the Fe<sup>0</sup> core/magnetite (Fe<sub>3</sub>O<sub>4</sub>) shell model proposed for this nZVI (4).

The EPM was measured as a function of pH immediately after washing the excess polyelectrolyte (at time = 0), and again after 8 weeks and 16 weeks of desorption time. The pH<sub>iep</sub> was stable after 8 weeks for bare or modified nZVI, so only 16-week results were plotted for clarity (Figure 2). It was anticipated that desorption would result in a less negative EPM of the particles. For PSS coated nZVI (Figure 2(a)), the EPM remained negative for pH 2–10 over the 16-week period, indicating that the PSS remains adsorbed, consistent with the batch desorption measurements. This was not the case for PAP (Figure 2(b)) and CMC (Figure 2(c)). After the excess polyelectrolyte was removed, the magnitude of EPM for both PAP and CMC modified nZVI decreased and the pH<sub>iep</sub> shifted

toward that of bare nZVI that had been aged for a similar time (Figure 2(d)). There was no significant change in EPM between the immediate washing and 16 weeks of desorption. The similarity of the PAP and CMC-coated nZVI aging behavior in the EPM experiments with that of bare nZVI indicates that the PAP and CMC desorbed from the particles, but this is inconsistent with the batch desorption measurements. The reason for the apparent similarity in EPM is not known, but desorption can be ruled out. Nevertheless, the pH<sub>iep</sub> remains relatively low for all the modified particles so that they should retain a net negative charge at typical groundwater pH. Because EPM could not be used to determine conclusively whether PAP and CMC remained adsorbed to the surface of the particles, mobility and sedimentation experiments were conducted as described next.

**Aggregation and Sedimentation.** Bare nZVI rapidly flocculates to micrometer-sized aggregates that sediment from suspension (10). The presence of surface coatings decreases the rate and extent of particle aggregation and sedimentation (12). Decreased sedimentation of modified particles relative to bare particles can therefore indicate the presence of the surface modifier. All the polyelectrolytes considered here decreased nZVI aggregation and sedimentation (Figure 3(a)), as expected. After 8 months of desorption, the PAP- and PSS-coated nZVI still showed significantly higher colloidal stability than bare nZVI aged under the same conditions (Figure 3(b)), indicating that polyelectrolyte remained adsorbed to the particle surface. The stability of CMC coated particles was only slightly better after 8 months of desorption than bare nZVI. In addition, CMC was the least effective stabilizer for freshly prepared samples (12). To determine how the partial polyelectrolyte desorption and corresponding changes in surface charge and aggregation behaviors would affect aged RNIP mobility, particle transport experiments in sand columns were conducted next. The aggregation and sedimentation measurement is only controlled by particle–particle interactions (including van der Waals attraction, magnetic attraction, electrostatic double layer repulsion, and electrosteric repulsion). Therefore, the sedimentation study is a simpler and less direct indication of nZVI transport, which includes both particle–particle interac-

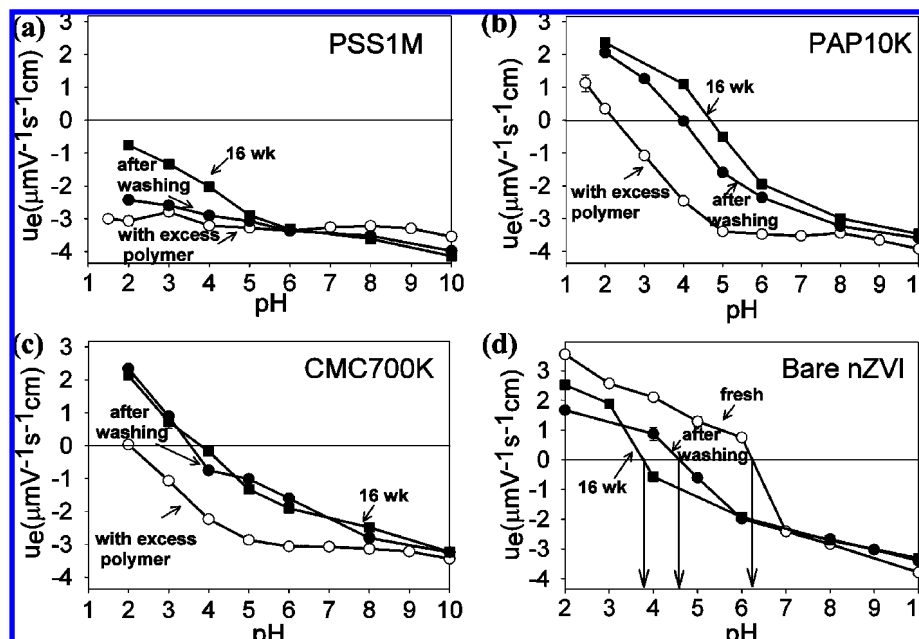


**FIGURE 2.** Electrophoretic mobility (EPM) vs. pH for nZVI modified by (a) PSS, (b) PAP and (c) CMC with excess polyelectrolyte (○), immediately after washing to remove excess polyelectrolyte (●), and after 16 weeks of desorption (■). (d) Bare nZVI treated identically and sampled at the same time points. The data shown are for PAP10K, PSS1M, and CMC700K, but the other molecular weights behaved similarly for each polyelectrolyte. Data collected after 8 weeks is the same for 16 weeks and are not included for clarity. nZVI concentration was 15 mg/L and ionic strength was controlled at 5 mM NaHCO<sub>3</sub>.

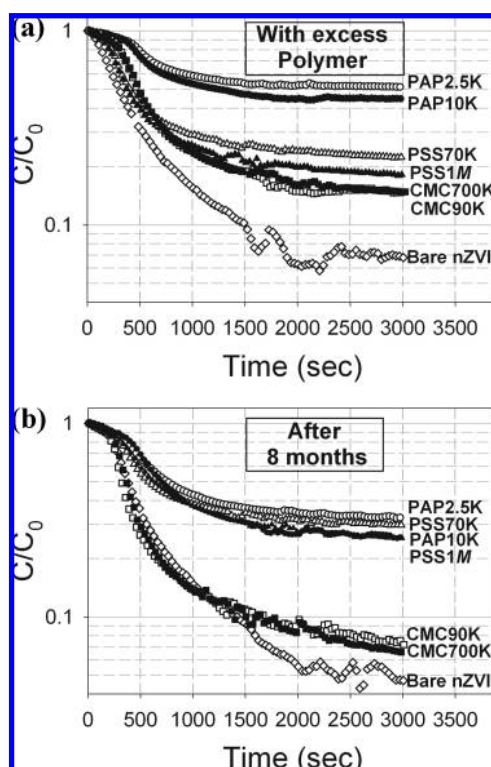


**FIGURE 3.** Sedimentation curves for bare and modified nZVI (800 mg/L) measured by UV-vis spectrophotometry at 508 nm in 1 mM NaHCO<sub>3</sub>. (a) With excess polyelectrolyte in solution in the case of modified nZVI at pH 9.5. (b) After 8 months of aging and desorption nZVI modified with PSS (low MW (△), high MW (▲)), PAP (low MW (○), high MW (●)), CMC (low MW (□), high MW (■)). Bare nZVI (◇) at pH 8.3 is also shown for comparison.

tion and particle-sand interaction, including the influence of fluid shear forces on aggregate-sand interactions.

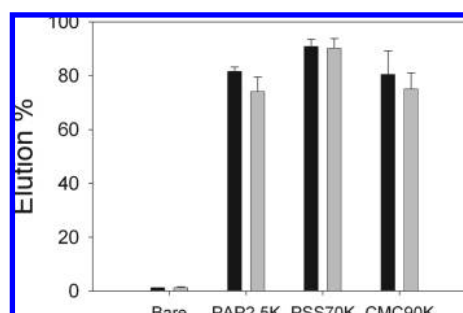


**FIGURE 4.** Percent mass of nZVI eluted through at 12.5-cm saturated silica sand column in 1mM NaHCO<sub>3</sub> for freshly modified particles with excess polymer at pH 9.5 (black bars) and after 8 months for aging and desorption at pH 8.3 (gray bars). Porosity is 0.33, pore water velocity is 1.08 × 10<sup>-3</sup> m/s, and particle concentration is 1 g/L. Silica sand (Agasco Corp., Hasbrouck Heights, NJ) had an average diameter of 300 µm.

**Transport Experiments.** Bare nZVI is immobile in sand columns at a concentration of 1 g/L, but adsorbed anionic polyelectrolytes increase mobility in sand columns (2, 3). Particle mobility therefore can be used as an indicator that polyelectrolyte remains adsorbed in an amount and conformation sufficient to inhibit deposition and straining. The percentage of bare, modified, and aged particles eluted from sand columns is shown in Figure 4. Whereas neither fresh nor aged bare nZVI was elutable, more than 70% of PAP, PSS, and CMC modified nZVI were eluted from the column even after the 8 months for desorption, indicating that polyelectrolyte remained adsorbed to the particles. CMC coated nZVI also showed high elutability even though its colloidal stability was close to the bare nZVI from the sedimentation. The partially desorbed CMC polymer layer may be ineffective at stabilizing nZVI against van der Waals and magnetically driven aggregation, but it may be still effective in minimizing adhesion to sand grains where no direct particle-sand magnetic attraction exists. Also, the shear force caused by the fluid flow can promote the disaggregation or dislodging of weakly adhered nZVI in

the sand column. This result is consistent with the batch desorption study and indicated that desorption of 20–30% of the surface coating after 8 months did not significantly decrease the potential for mobility in porous media. It also indicates the benefits of electrosteric repulsion. The downward drift in bare RNIP isoelectric point and corresponding increase in negative surface charge density near neutral pH conditions was not sufficient to mobilize bare RNIP. Simple electrostatic repulsion alone is insufficient to mobilize RNIP in sand columns.

## Environmental Implications

Slow desorption of polyelectrolyte from modified nZVI used for groundwater remediation has important implications for their application in the field. These results suggest that nZVI can potentially remain mobile for at least 8 months after emplacement depending on site hydrogeochemistry and on the type of coating material (3). This long-term mobility indicates a potential to reach sensitive receptors in the environment.

Recent reports indicate that the surface coatings affect the potential toxicity of nZVI (9). Coatings decreased toxicity by changing the surface charge or by decreasing oxidative stress. Because the coatings do not readily desorb, tests of mobility and toxicity should include the coated nZVI as these coatings may exist on particles for months or longer after release to the environment. These coatings are known to alter nZVI transport (2, 3) and toxicity characteristics (9) relative to the bare particles. Of course, these coatings may eventually be altered by biological or geochemical processes that remain to be investigated.

The bioavailability of adsorbed polyelectrolyte on the surface may be a key factor controlling the fate of surface modified nZVI because desorption is slow. The mobility, reactivity and toxicity may all be affected if the coatings can be degraded by microorganisms while attached to the nZVI. The microbial degradation of coatings needs to be studied further to fully understand the fate of surface modified nZVI.

The polyelectrolyte adsorbed to nZVI could be selected to serve as a carbon source to stimulate biological remediation of chlorinated organic compounds, especially in a carbon-limited environment. However, because the adsorbed polyelectrolyte is not readily desorbed, biostimulation will not occur unless microorganisms can degrade the attached polyelectrolyte. Strategies for enhancing biodegradation will therefore probably require an additional carbon source added to the injection solution such as excess free polymer or some other carbon source.

## Acknowledgments

We thank the Department of Defense through the Strategic Environmental Research and Development Program (W912HQ-06-C-0038), the U.S. Environmental Protection Agency (R833326), and the National Science Foundation (BES-068648 and EF-0830093) for funding.

## Supporting Information Available

Electrophoretic mobility with excess polymer present, the shift in the  $pH_{iep}$  for the bare nZVI and grain size distribution of sand. This material is available free of charge via the Internet at <http://pubs.acs.org>.

## Literature Cited

- (1) Li, X. Q.; Elliott, D. W.; Zhang, W. X. Zero-valent iron nanoparticles for abatement of environmental pollutants: Materials and engineering aspects. *Crit. Rev. Solid State Mater. Sci.* **2006**, *31* (4), 111–122.

- (2) Saleh, N.; Sirk, K.; Liu, Y. Q.; Phenrat, T.; Dufour, B.; Matyjaszewski, K.; Tilton, R. D.; Lowry, G. V. Surface modifications enhance nanoiron transport and NAPL targeting in saturated porous media. *Environ. Eng. Sci.* **2007**, *24* (1), 45–57.
- (3) Saleh, N.; Kim, H. J.; Phenrat, T.; Matyjaszewski, K.; Tilton, R. D.; Lowry, G. V. Ionic strength and composition affect the mobility of surface-modified  $Fe^0$  nanoparticles in water-saturated sand columns. *Environ. Sci. Technol.* **2008**, *42*, 3349–3355.
- (4) Liu, Y. Q.; Majetich, S. A.; Tilton, R. D.; Sholl, D. S.; Lowry, G. V. TCE dechlorination rates, pathways, and efficiency of nanoscale iron particles with different properties. *Environ. Sci. Technol.* **2005**, *39*, 1338–1345.
- (5) Liu, Y. Q.; Lowry, G. V. Effect of particle age ( $Fe^0$  content) and solution pH on NZVI reactivity:  $H_2$  evolution and TCE dechlorination. *Environ. Sci. Technol.* **2006**, *40*, 6085–6090.
- (6) Liu, Y.; Phenrat, T.; Lowry, G. V. Effect of TCE concentration and dissolved groundwater solutes on NUI-Promoted TCE dechlorination and  $H_2$  evolution. *Environ. Sci. Technol.* **2007**, *41*, 7881–7887.
- (7) Henn, K. W.; Waddill, D. W. Utilization of nanoscale zero-valent iron for source remediation - A case study. *Remediation* **2006**, *16* (2), 57–77.
- (8) Wiesner, M. R.; Lowry, G. V.; Alvarez, P.; Dionysiou, D.; Biswas, P. Assessing the risks of manufactured nanomaterials. *Environ. Sci. Technol.* **2006**, *40*, 4336–4345.
- (9) Phenrat, T.; Long, T. C.; Lowry, G. V.; Veronesi, B. Partial oxidation (“aging”) and surface modification decrease the toxicity of nanosized zerovalent iron. *Environ. Sci. Technol.* **2009**, *43*, 195–200.
- (10) Phenrat, T.; Saleh, N.; Sirk, K.; Tilton, R. D.; Lowry, G. V. Aggregation and sedimentation of aqueous nanoscale zerovalent iron dispersions. *Environ. Sci. Technol.* **2007**, *41*, 284–290.
- (11) Hoch, L. B.; Mack, E. J.; Hydutsky, B. W.; Hershman, J. M.; Skluzacek, I. M.; Mallouk, T. E. Carbothermal synthesis of carbon-supported nanoscale zero-valent iron particles for the remediation of hexavalent chromium. *Environ. Sci. Technol.* **2008**, *42*, 2600–2605.
- (12) Phenrat, T.; Saleh, N.; Sirk, K.; Kim, H. J.; Tilton, R. D.; Lowry, G. V. Stabilization of aqueous nanoscale zerovalent iron dispersions by anionic polyelectrolytes: adsorbed anionic polyelectrolyte layer properties and their effect on aggregation and sedimentation. *J. Nanopart. Res.* **2008**, *10* (5), 795–814.
- (13) He, F.; Zhao, D. Y. Manipulating the size and dispersibility of zerovalent iron nanoparticles by use of carboxymethyl cellulose stabilizers. *Environ. Sci. Technol.* **2007**, *41*, 6216–6221.
- (14) Kanel, S. R.; Nepal, D.; Manning, B.; Choi, H. Transport of surface-modified iron nanoparticle in porous media and application to arsenic(III) remediation. *J. Nanopart. Res.* **2007**, *9* (5), 725–735.
- (15) Sirk, K. M.; Saleh, N. B.; Phenrat, T.; Kim, H.-J.; Dufour, B.; Ok, J.; Golas, P. L.; Matyjaszewski, K.; Lowry, G. V.; Tilton, R. D. Effect of adsorbed polyelectrolytes on nanoscale zero valent iron particle attachment to soil surface models. *Environ. Sci. Technol.* **2009**.
- (16) Phenrat, T.; Liu, Y.; Tilton, R. D.; Lowry, G. V. Adsorbed polyelectrolyte coatings decrease  $Fe^0$  nanoparticle reactivity with TCE in water: conceptual model and mechanisms. *Environ. Sci. Technol.* **2009**, *43*, 1507–1514.
- (17) Fleer, G. J. C. S., M. A.; Scheutjens, J. M. H. M.; Cosgrove, T.; Vincent, B. *Polymers at Interfaces*; Chapman and Hall: London, 1993.
- (18) Pefferkorn, E.; Carroy, A.; Varoqui, R. Dynamic behavior of flexible polymer at a solid liquid interface. *J. Polym. Sci., Part B: Polym. Phys.* **1985**, *23* (10), 1997–2008.
- (19) O’Shaughnessy, B.; Vavylonis, D. Irreversible adsorption from dilute polymer solutions. *Eur. Phys. J. E.* **2003**, *11* (3), 213–230.
- (20) Shaffer, J. S.; Chakraborty, A. K. Dynamics of poly (methyl methacrylate) chains adsorbed on aluminum surfaces. *Macromolecules* **1993**, *26* (5), 1120–1136.
- (21) Vandesteeg, H. G. M.; Stuart, M. A. C.; Dekeizer, A.; Bijsterbosch, B. H. Polyelectrolyte adsorption - a subtle balance of forces. *Langmuir* **1992**, *8* (10), 2538–2546.
- (22) Dobrynin, A. V.; Rubinstein, M. Effect of short-range interactions on polyelectrolyte adsorption at charged surfaces. *J. Phys. Chem. B* **2003**, *107* (32), 8260–8269.
- (23) Wolterink, J. K.; Koopal, L. K.; Stuart, M. A. C.; Van Riemsdijk, W. H. Surface charge regulation upon polyelectrolyte adsorption, hematite, polystyrene sulfonate, surface charge regulation - Theoretical calculations and hematite-poly(styrene sulfonate) system. *Colloids Surf., A* **2006**, *291* (1–3), 13–23.
- (24) Bandara, J.; Mielczarski, J. A.; Kiwi, J. I. Molecular mechanism of surface recognition. Azo dyes degradation on Fe, Ti, and Al

- oxides through metal sulfonate complexes. *Langmuir* **1999**, *15* (22), 7670–7679.
- (25) Rochelle M. Cornell, U. S. *The Iron Oxides*. 2nd ed.; Oxford University Press: New York, 2000; p 361.
- (26) Yu, S.; Chow, G. M. Carboxyl group (-CO<sub>2</sub>H) functionalized ferrimagnetic iron oxide nanoparticles for potential bio-applications. *J. Mater. Chem.* **2004**, *14* (18), 2781–2786.
- (27) Kirwan, L. J.; Fawell, P. D.; van Bronswijk, W. In situ FTIR-ATR examination of poly(acrylic acid) adsorbed onto hematite at low pH. *Langmuir* **2003**, *19* (14), 5802–5807.
- (28) Hoogendam, C. W.; de Keizer, A.; Stuart, M. A. C.; Bijsterbosch, B. H.; Batelaan, J. G.; van der Horst, P. M. Adsorption mechanisms of carboxymethyl cellulose on mineral surfaces. *Langmuir* **1998**, *14* (14), 3825–3839.
- (29) Bacchin, P.; Bonino, J. P.; Martin, F.; Combacau, M.; Barthes, P.; Petit, S.; Ferret, J. Surface pre-coating of talc particles by carboxyl methylcellulose adsorption: Study of adsorption and consequences on surface properties and settling rate. *Colloids Surf, A* **2006**, *272* (3), 211–219.
- (30) Kenausis, G. L.; Voros, J.; Elbert, D. L.; Huang, N. P.; Hofer, R.; Ruiz-Taylor, L.; Textor, M.; Hubbell, J. A.; Spencer, N. D. Poly-(L-lysine)-g-poly(ethylene glycol) layers on metal oxide surfaces: Attachment mechanism and effects of polymer architecture on resistance to protein adsorption. *J. Phys. Chem. B* **2000**, *104* (14), 3298–3309.
- (31) Tadros, T. F. *The Effect of Polymers on Dispersion Properties*; Academic Press: New York/London, 1983; p 81.
- (32) Ramachandran, R.; Somasundaran, P. Competitive adsorption of polyelectrolytes - a size exclusion chromatographic study. *J. Colloid Interface Sci.* **1987**, *120* (1), 184–188.
- (33) Cosgrove, T.; Obey, T. M.; Vincent, B. The configuration of sodium poly(styrene sulfonate) at polystyrene solution interfaces. *J. Colloid Interface Sci.* **1986**, *111* (2), 409–418.
- (34) Blokhuis, A. M.; Djurhuus, K. Adsorption of poly(styrene sulfonate) of different molecular weights on alpha-alumina: Effect of added sodium dodecyl sulfate. *J. Colloid Interface Sci.* **2006**, *296* (1), 64–70.
- (35) Velegol, S. B.; Tilton, R. D. A connection between interfacial self-assembly and the inhibition of hexadecyltrimethylammonium bromide adsorption on silica by poly-L-lysine. *Langmuir* **2001**, *17* (1), 219–227.
- (36) Vanderschuer, H. A.; Lyklema, J. A lattice theory of polyelectrolyte adsorption. *J. Phys. Chem.* **1984**, *88* (26), 6661–6667.
- (37) Chibowski, S.; Wisniewska, M. Study of electrokinetic properties and structure of adsorbed layers of polyacrylic acid and polyacrylamide at Fe<sub>2</sub>O<sub>3</sub>-polymer solution interface. *Colloids Surf, A* **2002**, *208* (1–3), 131–145.
- (38) Sukhishvili, S. A.; Granick, S. Kinetic regimes of polyelectrolyte exchange between the adsorbed state and free solution. *J. Chem. Phys.* **1998**, *109* (16), 6869–6878.

ES802978S